Original Article PROGRESS in MEDICAL PHYSICS Vol. 26, No. 3, September, 2015
http://dx.doi.org/10.14316/pmp.2015.26.3.119

Study of Motion-induced Dose Error Caused by Irregular Tumor Motion in Helical Tomotherapy

Min-Seok Cho*†, Tae-Ho Kim*†, Seong-Hee Kang*†, Dong-Su Kim*†, Kyeong-Hyeon Kim*†, Geum Seong Cheon*†, Tae Suk Suh*†

*Department of Biomedical Engineering, and †Research Institute of Biomedical Engineering, College of Medicine, The Catholic University of Korea, Seoul, Korea

The purpose of this study is to analyze motion-induced dose error generated by each tumor motion parameters of irregular tumor motion in helical tomotherapy. To understand the effect of the irregular tumor motion, a simple analytical model was simulated. Moving cases that has tumor motion were divided into a slightly irregular tumor motion case, a large irregular tumor motion case and a patient case. The slightly irregular tumor motion case was simulated with a variability of 10% in the tumor motion parameters of amplitude (amplitude case), period (period case), and baseline (baseline case), while the large irregular tumor motion case was simulated with a variability of 40%. In the phase case, the initial phase of the tumor motion was divided into end inhale, mid exhale, end exhale, and mid inhale; the simulated dose profiles for each case were compared. The patient case was also investigated to verify the motion-induced dose error in 'clinical-like' conditions. According to the simulation process, the dose profile was calculated. The moving case was compared with the static case that has no tumor motion. In the amplitude, period, baseline cases, the results show that the motion-induced dose error in the large irregular tumor motion case was larger than that in the slightly irregular tumor motion case or regular tumor motion case. Because the offset effect was inversely proportion to irregularity of tumor motion, offset effect was smaller in the large irregular tumor motion case than the slightly irregular tumor motion case or regular tumor motion case. In the phase case, the larger dose discrepancy was observed in the irregular tumor motion case than regular tumor motion case. A larger motion-induced dose error was also observed in the patient case than in the regular tumor motion case. This study analyzed motion-induced dose error as a function of each tumor motion parameters of irregular tumor motion during helical tomotherapy. The analysis showed that variability control of irregular tumor motion is important. We believe that the variability of irregular tumor motion can be reduced by using abdominal compression and respiratory training.

Key Words: Motion-induced dose error, Tumor motion, Helical tomotherapy

Introduction

Tumor motion caused by respiration produces motion-induced dose errors in radiation therapy.[1-3] The motion-induced dose error presents additional complications in helical tomotherapy, as the tumor motion interacts with the couch motion.[4,5] Owing to the tumor motion, the treatment field does not reach the tumor region constantly, and repeatedly shifts in and out of the tumor area.[6,7] This effect prevents the delivery of the planned dose to the tumor region.[8,9] Typically, gating or tracking techniques are used to solve this problem in LINAC or cyberknife.[10-12] However, the use of such techniques is limited in helical tomotherapy, as the gantry and couch continuously move during the treatment.

This work was supported by the Radiation Technology R&D program (No. 2013M2A2A7043498) and the Mid-career Researcher Program (2014R1A2A1A10050270) through the National Research Foundation of Korea funded by the Ministry of Science, ICT&Future Planning and Development of the core technology for integrated therapy devices based on real-time MRI guided tumor tracking, Information and Communication Technologies (ICT) & Future Planning (MSIP) (Grant No. 2009-00420).
Received 30 July 2015, Revised 28 August 2015, Accepted 7 September 2015
Correspondence: Tae Suk Suh (suhsanta@catholic.ac.kr)
Tel: 82-2-2258-7232, Fax: 82-2-2258-7506
This is an Open-Access article distributed under the terms of the Creative Commons Attribution Non-Commercial License (http://creativecommons.org/licenses/by-nc/4.0) which permits unrestricted non-commercial use, distribution, and reproduction in any medium, provided the original work is properly cited.

Many previous studies have focused on this issue.

Dose profiles according to the changes of the field widths and gantry rotation periods have been reported.[5] As a result of this study, 5 cm of field width exhibited better gamma passing rates than 1 cm and 2.5 cm widths in the gamma comparisons with 2% dose discrepancy and 2 mm distance-to-agreement. In a different study focused on couch motion,[7] the couch motion was varied within a range of values, and the effects on the dose profiles were assessed. Furthermore, different dose profiles in relation to the initial phase of the tumor motion have been shown.[6] Many studies related to this issue have used 'regular' and 'sinusoidal' waveforms to represent the tumor motion, and these limitations have been shown to be significant. However, in reality, the tumor motion has an 'irregular' waveform. Therefore, the aim of this study is to analyze motion-induced dose error generated by tumor motion parameters of irregular tumor motion in helical tomotherapy.

Materials and Methods

1. Theory to acquire the dose profile

To understand the effects of the irregular tumor motion of a target, a simple one-dimensional model was simulated (Fig. 1). The target was modeled as a rigid line. The treatment field (W), which is blocked by two jaws, represented the treatment field exposed in helical tomotherapy. We denoted the positions of the treatment field caused by the couch motion and tumor motion as 'x_s' and 'x_r', respectively. A more detailed explanation is presented in the following section.

1) Tumor coordinate system: In this study, a tumor coordinate system was used to explain the acquisition process of the dose profile and analyze the motion-induced dose errors.[4] The tumor coordinate system is different from the room coordinate system normally used. The treatment room is the standard in the room coordinate system; therefore, the target is moved by the tumor motion, and the couch is moved in the superior-inferior (SI) direction with constant velocity (Fig. 2a). Conversely, as the tumor is the standard in the tumor coordinate system (Fig. 2b), the target dose does not move while the treatment field undergoes a complex motion.

2) Static dose acquisition: To produce the dose profiles (Fig. 1), a static dose was acquired by using a Hi-Art tomotherapy unit (TomoTherapy, Inc., Madison, WI, USA). The tomotherapy had a 'static mode' that prevented the movement of gantry and couch during the beam exposure. A cylindrical 'cheese' phantom (TomoTherapy, Inc., Madison, WI, USA;

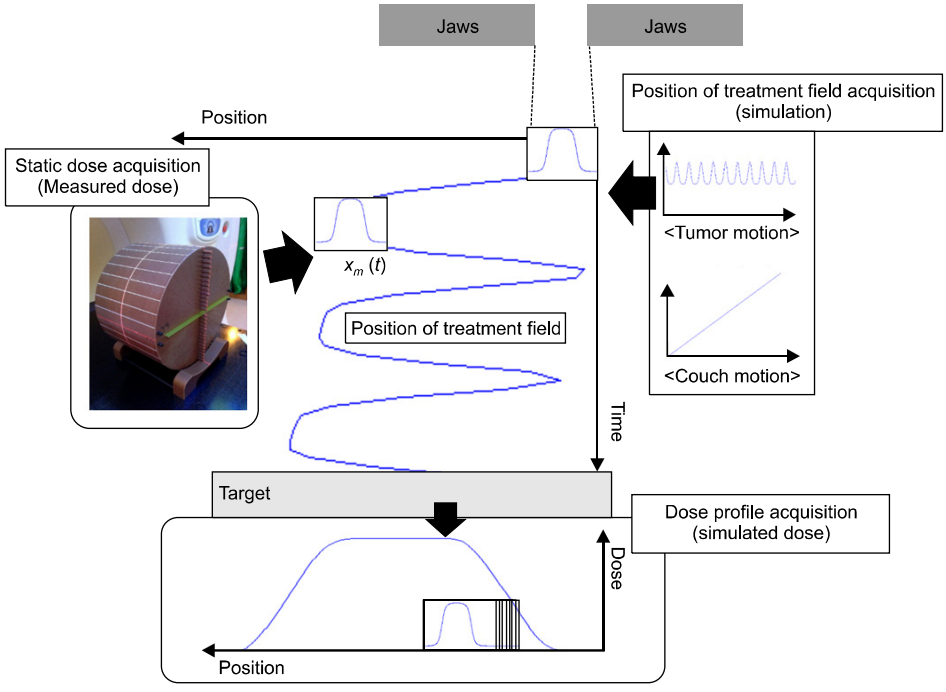

Fig. 1. Schematic of acquiring the dose profile.

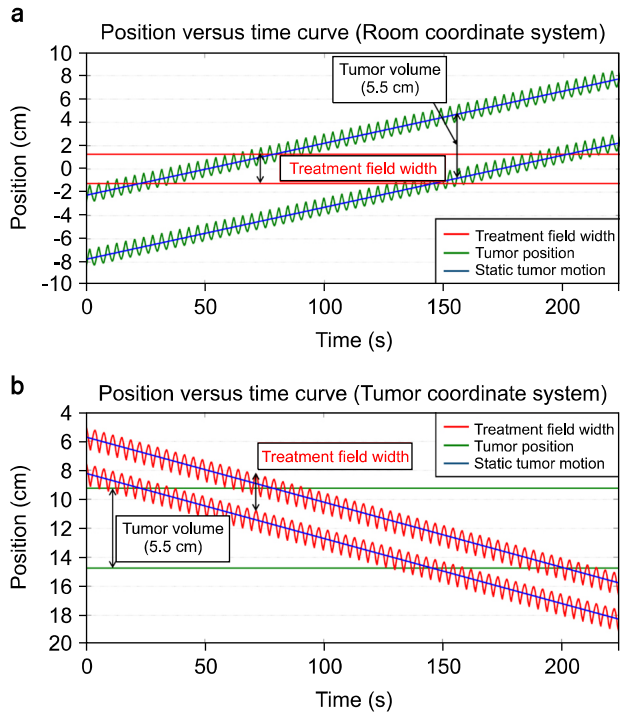

Fig. 2. Position versus time curve of the treatment field in the (a) room coordinate system and (b) tumor coordinate system.

length: 18 cm, diameter: 30 cm) was used to acquire the static dose in the 'patient-like' condition. The cheese phantom was placed in the isocenter of the tomotherapy. A Gafchromic EBT2™ film (Ashland Inc., Covington KY) was inserted in the cheese phantom and was exposed by static mode of tomotherapy. More details on the conditions used in the measuring process are given in Table 1. The film was kept for 24 h at controlled pressure and humidity prior to scan. A VXR Dosimetry PRO Advantage (RED) Film Digitizer (Vidar Systems Corporation, Hendon, Virginia) device and VIDAR TWAIN version 5.2 software (Vidar Systems Corporation, Hendon, Virginia) were used to scan the film image. The resolution of the scanner was 71 dots per inch (DPI), and the scanned range was 14×17 inches. All the scanned images were calibrated by a film calibration curve determined by using films exposed to the known doses of 74.64, 148.14, 222.21, 295.71, 369.2, 442.7, 516.2, 589.12, and 662.62 cGy. The American Association of Physicists in Medicine (AAPM) Task Group report No. 69 report and many related papers were considered during the film measurement.[13-15] SI direction curves of the calibrated image were collected, and a curve at the isocenter was selected

Table 1. Experimental conditions used to acquire the static dose.

Part	Parameters	Experimental condition
Gantry	Source to axis distance (SAD)	85 cm
	Beam delivery mode	Static mode
	Beam energy	6 MV
	Treatment field width	2.5 cm
	Angle of exposed beam	90°
Phantom	Type of phantom	Cheese phantom
	Centered point	Isocenter
Film	Type of film	Gafchromic EBT2
	Expiration date	June 2015
	Lot number	06241301

to determine the 'static dose' (φ). ImageJ v1.48 (US National Institutes of Health) and Matlab (version R2012b, Mathworks, Natick, MA, USA) softwares were used in the process of calibration and acquiring static dose.

3) Position of treatment field acquisition: The position of the treatment field, which is caused by the couch motion x_s, can be written as a function of time t:

$$x_s(t) = x_0 - vt \quad (1)$$

where x_0 is the initial position at which the static dose starts to accumulate and v is the velocity of the couch. As a tumor coordinate system was used, the position of the radiation field moved in opposite direction to that of the couch motion (Fig. 2).

To improve the accuracy, all the tumor motions were generated by an internet accessible respiratory trace generator (RTG) (http://www.ucalgary.ca/rop/Research/Respiratory).[16] In addition, the RTG could produce specific tumor motions for which a specific tumor motion parameter was irregular. For example, to produce tumor motion for which only the amplitude is irregular, the RTG could generate a tumor motion with an amplitude in the range of 1.35∼1.65 cm and a period of 4 s. As for x_s, the opposite direction of the tumor motion (x_r) was used to calculate the position of the treatment field.

The position of the treatment field x_m caused by the couch motion and tumor motion was calculated as a function of time t:

$$x_m(t) = x_s(t) + x_r(t) \quad (2)$$

where $x_s(t)$ is the same as that in Equation (1) and $x_r(t)$ is the tumor motion produced by the RTG (Fig. 2) and $x_r(t)$ is the position of the treatment field caused by the tumor motion.

4) Dose profile acquisition: To acquire the dose profile, the position of the treatment field was changed as a function of time, and the static doses were cumulated (Fig. 1). The dose profile can be expressed as:

$$\phi = \sum_{t=T_{in}}^{T_{out}} \varphi(x_m(t)) \quad (3)$$

where ϕ is dose profile, $\varphi(x_m(t))$ is static dose at the position of the treatment field x_m (same as that in Equation (2)), T_{in} is the time at which the static dose started accumulating, and T_{out} is the time at which the static dose stopped accumulating.

2. Methods

The resulting dose profile depended on four tumor motion parameters, i.e., amplitude, period, baseline, and initial phase. The moving case (experimental group) and static case (control group) were set to confirm the motion-induced dose error. The moving case was set to produce a dose profile that has a motion-induced dose error; the static case was acquired for comparison with the moving case. The moving cases were divided in two categories. One category was set to confirm the dose profile according to the variability of the tumor motion parameters in the irregular tumor motion. Based on the regular tumor motion amplitude of 1.5 cm and a period of 4 s, each tumor motion parameter was set to a percent variability of 10% (slightly irregular tumor motion case) and 40% (large irregular tumor motion case) in tumor motion amplitude (amplitude case), period (period case), and baseline (baseline case). For example, the slightly irregular tumor motion in the period case was set to a tumor motion with amplitude of 1.5 cm and period between 3.6 s and 4 s. A percent variability of 10% was assumed for a tumor motion generated by normal breathing and 40% for a tumor motion generated by deep breathing.[17] The phase case concerned the initial phase of the tumor motion, which was divided into end inhale, mid exhale, end exhale, and mid inhale. The tumor motions of a regular tumor motion case and a patient case were used to compare the discrepancy effects of the tumor motion. The second category comprises the patient case, in which all the tumor motion parameters are irregular.

Table 2. Helical tomotherapy parameters and target volume information used in the simulation.

Parameters	Experimental condition
Total number of rotation	Static mode
Gantry rotation period (Tg)	16 s
Projection number per rotation	51 times
Treatment field width	2.5 cm
Pitch factor	0.287
PTV dimension (Cylindrical shape)	Isocenter

The tumor motion for each moving case was calculated according to Equation (2). The dose profiles were acquired by adding the calculated position of the treatment field (Equation (3)). More details on the conditions adopted to calculate the dose profile are given in Table 2.

To analyze the motion-induced dose error, the dose profiles were evaluated for all the points. The amplitude, period, baseline, and patient cases were compared with the static case, and the maximum dose discrepancy between the moving case and static case was investigated. In the phase case, the end inspiration, mid expiration, end expiration, and mid inspiration phases of the tumor motion were compared. The position versus time curve of the treatment field was used to investigate the causes of the motion-induced dose error (Fig. 2).

Results and Discussion

1. Motion-induced dose errors generated by tumor motion parameters (amplitude case, period case, baseline case)

Fig. 3a shows the motion-induced dose error in the amplitude case. The dose profiles in the regular tumor motion case (green line), slightly irregular tumor motion case (red line), and large irregular tumor motion case (cyan line) were compared with the static case (blue line). The maximum dose discrepancies observed were 3.3% in the regular tumor motion case, 3.0% in the slightly irregular tumor motion case, and 4.6% in the large irregular tumor motion case. Fig. 3b was used to analyze the cause of the motion-induced dose error in the amplitude case. Owing to the tumor motion, ‘in’ and ‘out’

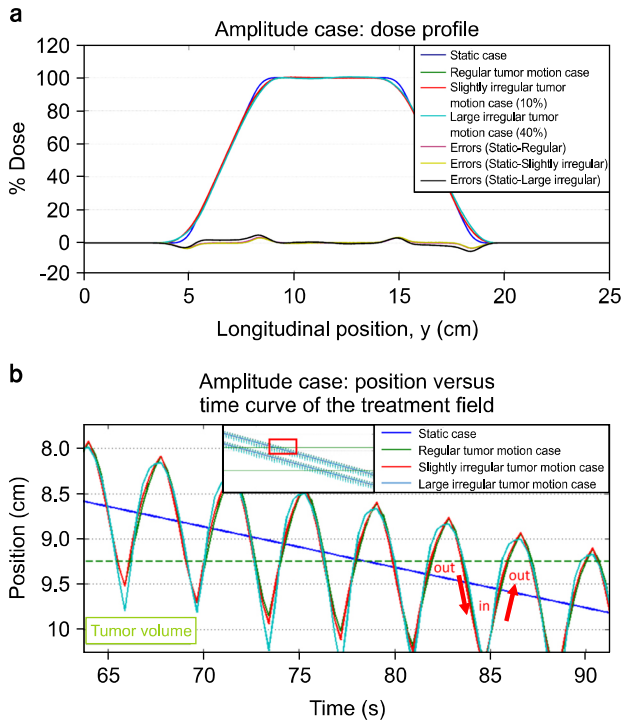

Fig. 3. (a) Dose profiles in the amplitude case. (b) Position versus time curve in the amplitude case.

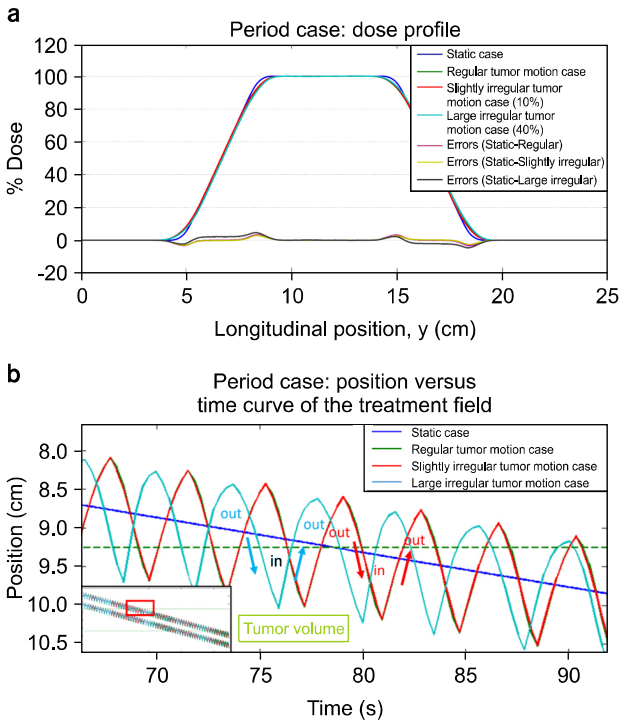

Fig. 4. (a) Dose profiles in the period case. (b) Position versus time curve in the period case.

areas were generated by the curves of the static case and moving case. This effect caused an accumulation of the static dose at different positions. In the regular tumor motion case, the 'in' and 'out' areas were identical. Therefore, an offset effect was generated, allowing the reduction of the motion-induced dose error. However, in the amplitude case, the tumor motion amplitude varied irregularly and appeared smaller or larger than that in the regular tumor motion case. Consequently, smaller, or larger, 'in' and 'out' areas were generated. This effect reduced the offset effect, and the generated motion-induced dose error was larger than that observed in the regular tumor motion case.

Fig. 4a shows the motion-induced dose error in the period case. The maximum observed dose discrepancy for the slightly irregular motion case (red line) was 3.1%, whereas, for the large irregular motion case (cyan line), was 4.3%, confirming a tendency of the dose profile similar to that observed in the amplitude case. In the amplitude and period cases, no large discrepancy was observed between the regular tumor motion case and the slightly irregular tumor motion case. Fig. 4b examines the reason behind the motion-induced dose error generated in the period case. A larger 'in' area was produced by a larger period and a smaller 'out' area was produced by a smaller period. This effect reduced the offset effect.

Fig. 5a shows the effects on the motion-induced dose error in the baseline case. In the slightly irregular motion case, the maximum dose discrepancy was 6.9%, whereas, in the large irregular motion case, the maximum error was 15.9%. In the large irregular tumor motion case, the motion-induced dose error was greater than that in the slightly irregular tumor motion case. In the baseline case, the effects observed in the amplitude case and period case were generated at the same time. Therefore, we believe that the baseline drift can have a significant impact.

2. Motion-induced dose errors according to the initial phase

The motion-induced dose error can also be observed in the

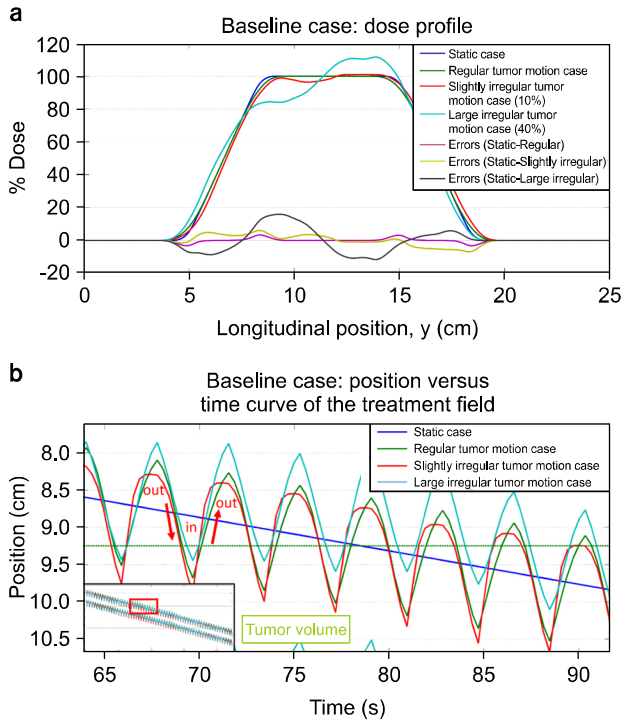

Fig. 5. (a) Dose profiles in the baseline case. (b) Position versus time curve in the baseline case.

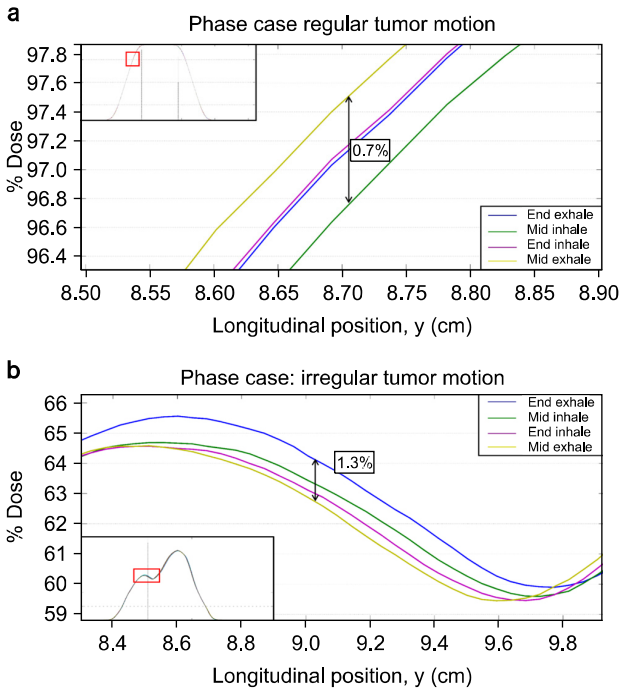

Fig. 6. Dose profiles in the phase case (end inspiration, mid expiration, end expiration, and mid inspiration). The tumor motion was divided in (a) regular tumor motion case and (b) irregular tumor motion case.

initial phase of a tumor motion. Fig. 6 shows that the dose profile changed depending on the different initial phase of a tumor motion. For a regular tumor motion, the maximum dose discrepancy between the initial phases of a tumor motion was approximately 0.7%, whereas a value of 1.3% was observed for the irregular motion. A different dose discrepancy was observed at different positions of the curve. In the patient case, the motion-induced dose error was larger than that in the regular tumor motion case. To reduce the motion-induced dose error, the effect of the tumor motion initial phase should be considered.

3. Motion-induced dose errors in the patient case

In the patient case, the effects of the tumor motion parameters (amplitude, period, and baseline) generated motion-induced dose errors (Fig. 7a). A maximum 15.0% dose error was observed in the patient case. Fig. 7b reveals the reason of the motion-induced dose error. Owing to the effects of the tumor motion parameters, the offset effect was not generated in the regular tumor motion case, causing a significant motion-induced dose error.

To reduce the motion-induced dose errors, it is necessary to reduce the variability of the tumor motion parameters. The current clinically applicable methods based on abdominal compression and respiratory training seem to provide appropriate solutions to minimize the tumor motion.

In this study, we analyzed the motion-induced dose error generated by irregular tumor motion. The motion-induced dose error observed in the irregular tumor motion case was larger than those seen in the slightly irregular tumor motion and regular tumor motion cases. Consequently, we believe that the motion-induced dose error generated by a “large irregular” tumor motion can be greater than that of a regular tumor motion. Even though this result was acquired by simplifying the treatment field geometry and tumor motion, it still helps intuitively understand the relationship between the irregular tumor motion and motion-induced dose error.

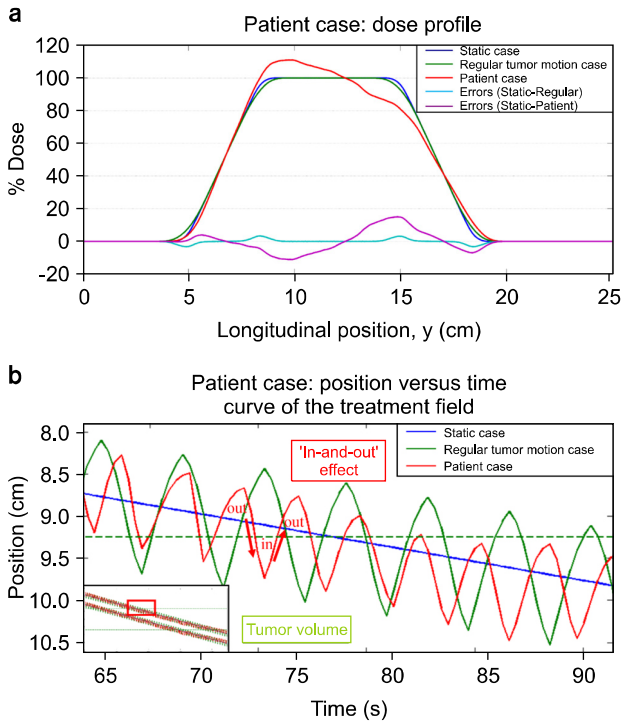

Fig. 7. (a) Dose profiles in the patient case: no tumor motion case, regular tumor motion case, and real tumor motion case were compared. (b) Position versus time curve in the patient case.

Conclusion

In this study, motion-induced dose error as a function of each tumor motion parameters of irregular tumor motion during helical tomotherapy was investigated. The analysis showed that variability control of irregular tumor motion is important. We believe variability of irregular tumor motion can be reduced by using abdominal compression and respiratory training. This study may help understand the effects of the tumor motion parameters on the dose profile.

References

1. **Cedric X Yu, David A Jaffray, John W Wong**: The effects of intra-fraction organ motion on the delivery of dynamic intensity modulation. Phys. Med. Biol. 43(1):91-104 (1998).
2. **Bortfeld, Thomas, Steve B. Jiang, Eike Rietzel**, Effects of motion on the total dose distribution. Semin. Radiat. Oncol. 14(1):41-51 (2004).
3. **Sung Kyu Kim, Min Kyu Kang, Ji Woon Yea, Se An Oh**: Dosimetric evaluation of a moving tumor target in intensity-modulated radiation therapy (IMRT) for lung cancer patients. J. Korean Phys. Soc. 63(1):67-70 (2013).
4. **B. Kim, J. Chen, T. Kron and J. Battista**: Motion-induced dose artifacts in helical tomotherapy. Phys. Med. Biol. 54(19): 5707-5734 (2009).
5. **M. Klein, S. Gaede and S. Yartsev**: A study of longitudinal tumor motion in helical tomotherapy using a cylindrical phantom. J. Appl. Clin. Med. Phys 14(2):52-61 (2013).
6. **J. H. Lewis and S. B. Jiang**: A theoretical model for respiratory motion artifacts in free-breathing CT scans. Phys. Med. Biol. 54(3):745-755 (2009).
7. **M. W. Kissick, J. Fenwick, J. A. James, et al**: The helical tomotherapy thread effect. Med. Phys. 32(5):1414-1423 (2005).
8. **J. N. Yang, T. R. Mackie, P. Reckwerdt, J. O. Deasy and B. R. Thomadsen**: An investigation of tomotherapy beam delivery. Med. Phys. 24(3):425-436 (1997).
9. **Brian Kanagaki, Paul W Read, Janelle A Molloy, James M Larner, Ke Sheng**: A motion phantom study on helical tomotherapy: the dosimetric impacts of delivery technique and motion. Phys. Med. Biol. 52(1):243-255 (2007).
10. **A. Schweikard, H. Shiomi and J. Adler**: Respiration tracking in radiosurgery. Med. Phys. 31(10):2738-2741 (2004).
11. **P. Giraud, E. Morvan, L. Claude, et al**: Respiratory Gating Techniques for Optimization of Lung Cancer Radiotherapy. J. Thorac. Oncol. 6(12):2058-2068 (2011).
12. **Martin J Murphy**: Tracking moving organs in real time. Semin. Radiat. Oncol. 14(1):91-100 (2004).
13. **AAPM TG-69 Report**: Radiographic film for megavoltage beam dosimetry, Sujatha Pai (2007).
14. **Martina Fuss, Eva Sturtewagen, Carlos De Wagter, Dietmar Georg**: Dosimetric characterization of GafChromic EBT film and its implication on film dosimetry quality assurance. Phys. Med. Biol. 52(14):4211-4225 (2007).
15. **Bart D. Lynch, Jakub Kozelka, Manisha K. Ranade, et al**: Important considerations for radiochromic film dosimetry with flatbed CCD scanners and EBT GAFCHROMIC ® film. Jonathan G. Li, William E. Simon, James F. Dempsey, Med. Phys. 33(12):4551-4556 (2006).
16. **Sarah Quirk, Nathan Becker, and Wendy Smith**: External respiratory motion: Shape analysis and custom realistic respiratory trace generation. Med. Phys. 39(8):4999-5003 (2012).
17. **AAPM TG-76 Report**: The management of respiratory motion in radiation oncology, P. J. Keall (2006).

나선형 토모테라피에서 불규칙적인 호흡으로 발생되는 움직임에 의한 선량 오차에 대한 연구

*가톨릭대학교 의과대학 의공학교실, †가톨릭대학교 생체의공학연구소

조민석*† · 김태호*† · 강성희*† · 김동수*† · 김경현*† · 천금성*† · 서태석*†

본 연구에서는 불규칙적인 종양의 움직임에서 각각의 움직임 파라미터에 의해 발생되는 토모테라피 장비의 선량 오차 특성을 분석하여, 각각의 파라미터가 선량에 미치는 효과를 확인하기 위해 간소화된 이론 모델을 적용, 시뮬레이션 분석을 수행하고자 한다. 간단한 분석적인 모델이 tumor motion parameters에 의한 motion-induced dose error를 분석하기 위해 사용되었다. 분석적인 모델은 실제 tomotherapy 장비를 이용한 static dose와 Simulated tumor motion를 이용하여 dose profile을 획득하는 것이다. 본 연구에서는 Static dose를 얻기 위해 Hi-art tomotherapy unit을 이용하였다. Simulated tumor motion은 internet accessible respiratory trace generator (RTG) program을 이용하여 획득되었다. 종양의 움직임은 불규칙한 정도가 큰 케이스와 작은 케이스, 실제 환자의 종양 움직임을 모사한 케이스로 구분하였다. 불규칙도가 작은 케이스의 경우 종양의 진폭, 주기, 베이스라인 등 종양 움직임 파라미터에 10% 변동을 인가 하였으며, 불규칙도가 큰 케이스의 경우 40%의 변동을 인가 하였다. 위상변동 케이스의 경우 종양의 초기위상이 end inhale, mid exhale, end exhale, and mid inhale으로 나뉘어 졌고, 시뮬레이션을 통해 획득된 각각의 선량분포결과가 비교되었다. 또한, 환자 케이스에서는 임상과 동일한 조건에서의 종양 움직임을 인가하여 선량 오차를 획득하였다. 종양의 움직임에 의한 선량은 시뮬레이션 과정을 통해 계산되었으며 이를 종양의 움직임이 없는 케이스와 비교하여 종양 움직임이 선량에 미치는 영향을 확인했다. 진폭, 주기, 베이스라인 등 종양 움직임 파라미터가 불규칙하게 변하는 경우, 종양이 불규칙하게 움직이는 케이스의 경우 불규칙도가 큰 케이스의 경우가 불규칙도가 작은 케이스와 규칙적으로 움직이는 케이스보다 더 큰 선량오차가 발생하였다. 상쇄 효과는 종양움직임의 불규칙성에 반비례하기 때문에, 종양 움직임의 불규칙성이 큰 케이스의 경우 불규칙성이 작은 케이스, 종양의 움직임이 규칙적인 케이스에 비해 더 적은 상쇄 효과가 발생하였다. 위상변동 케이스의 경우, 불규칙한 종양의 움직임 케이스에서 규칙적인 움직임 케이스보다 더 큰 선량 차이가 관찰되었고, 또한 환자케이스에서 규칙적인 종양의 움직임의 경우보다 더 큰 선량의 차이가 발견되었다. 본 연구에서는 불규칙적인 종양의 움직임에서 각각의 움직임 변수들의 불규칙성에 따른 발생되는 토모테라피에서의 선량 오차 특성을 분석하였다. 본 연구의 결과를 통해 불균일한 종양 움직임의 불규칙성을 제어하는 것에 대한 중요성을 확인할 수 있었고, 이러한 불균일성의 제어의 경우 복부 압박이나 호흡 훈련을 통해 해결이 가능할 것으로 생각된다.

중심단어: 운동유도 선량오차, 종양 움직임, 나선형 토모테라피